Journal of Materials Chemistry C

Accepted Manuscript

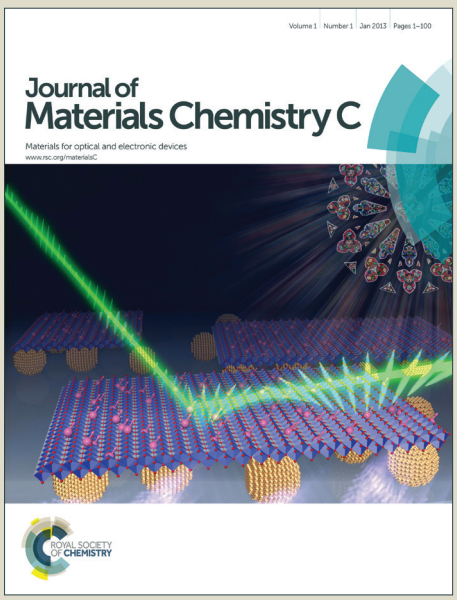

ROYAL SOCIETY OF CHEMISTRY

www.rsc.org/materialsC

Journal Name Journal of Materials Chemistry C Dynamic Article Links ►

Cite this: DOI: 10.1039/c0xx00000x

www.rsc.org/xxxxxx

ARTICLE TYPE

Sovothermal synthesis of $Co_xFe_{3-x}O_4$ spheres and their microwave absorption properties

Renlong Ji, Chuanbao Cao,* Zhuo Chen, Huazhang Zhai and Ju Bai

$Co_xFe_{3-x}O_4$ (x=0-1) spheres are synthesized via solvothermal reaction using ethylene glycol (EG) as solvent. They are characterized and the results show that the prepared spheres are mainly 300-500 nm in diameter and constituted by small grains. For the EG solution containing stoichiometric ingredients (atomic ratio of Co^{2+}:Fe^{3+}=1:2), the obtained spheres are $Co_{0.9}Fe_{2.1}O_4$ at 200°C (sphere A) and $Co_{0.74}Fe_{2.26}O_4$ (sphere B) at 300°C, whose crystallite is 23 nm and 30 nm in size respectively. VSM measurements reveal improved properties with sphere B. The variation of complex permittivity and permeability for different composite (75% mass ratio of spheres) has been studied as a function of frequency. The calculated reflectivity indicates that the composite containing sphere A displays better microwave absorption capability. The minimum reflection loss reaches -41.089 dB at 12.08 GHz and the matching thickness is 2 mm. Dielectric loss contributes even more than magnetic loss in the frequency range of 3 -14 GHz. The synergistic effect of dual losses makes the submicrosphere a promising absorbent in X and Ku bands. The composite consisting of spheres B is inferior in dielectric property owing to the ferrous ions migration from octahedral to tetrahedral sites and big crystallites lacking defects. After calcination treatment of the spheres at 700°C, the dielectric loss turns out to be little due to the disappeared $Fe^{2+} \leftrightarrow Fe^{3+}$ pairs in adjacent octahedral sites and loss of defects. Variation of cobalt ratio in spheres can change the resonance frequency and crystallinity of the spheres, and ultimately the minimum reflection loss and corresponding frequency band. The microwave absorption properties of mixed magnetite and cobalt ferrite spheres are influenced by the cationic stoichiometry and crystalline integrity.

1 Introduction

Microwave absorptive materials have been widely used in military stealth technique and civilian electromagnetic wave (EMW) protection. They are dielectric, conductive, magnetic monophasic material or a composite of them.[1-5] The practical application claims for relevant characteristics such as high strength, wide band, small thickness and lightweight.[6] Magnetic metals and ferrites play a leading role in this research area. On account of the corrosion susceptibility of metals, ferrites are the promising candidates as microwave absorbers due to their excellent chemical stability. They can be classified into three categories which are spinels, garnets and hexaferrites. The garnets are gyromagnetic materials and can be used in microwave isolator, phase shifter, circulator etc, which require least magnetic and dielectric losses.[7] Hexagonal ferrites have high saturation magnetization and large anisotropy field which result in high resonance frequency as microwave absorbents.[8,9] Cobalt ferrite is a kind of spinel structure material with moderate saturation magnetization but fairly high magnetocrystalline anisotropy (less than hexaferrites'), and large magnetostrictive coefficient owing to the introduction of cobalt atoms.[10,11] The material has been widely used as magnetic and magneto-optical recording medium.[12] Magnetite and maghemite have been studied a lot as soft magnetic spinels and microwave absorbents.[3,13-15] However, the microwave attenuation mechanism of cobalt ferrite are not fully understood. P.C. Fannin *et al*. have reported microwave absorbent properties of nanosized cobalt ferrite powders prepared by coprecipitation and subjected to different thermal treatments.[10] Asghari Maqsood *et al*. have reported $Ni_{(1-x)}Co_{(x)}Fe_2O_4$ ($0.0 \leqslant x \leqslant 0.5$) nanoferrites synthesized by the same route.[16] Wuyou Fu *et al*. have fabricated hollow glass microspheres coated with cobalt ferrite.[17] As a ferrimagnetic material, stoichiometric cobalt ferrite coprecipitated in a strong alkaline shows excellent magnetic property but not good dielectric property. The absorbing performance of cobalt ferrite mainly depends on the magnetic loss. Its dielectric loss is almost negligible.[18] We know that the microwave attenuation performance of absorbents is determined by the combination of dual losses. Either loss contributes partially to the whole. The synergistic effect is the product instead of sum of them. Some reports in the literature remedy this drawback through compounding cobalt ferrite with other materials.[19-22] In fact, its dielectric property can be tuned by the preparation

Research Center of Materials Science, Beijing Institute of Technology, 100081 Beijing, China
**Author to whom correspondence should be addressed. E-mail: cbcao@bit.edu.cn. Tel: +86-10-6891-3792. Fax: +86-10-6891-3792*

methodology. It is evidenced in this paper that dielectric loss of cobalt ferrite fabricated under proper condition is even more than magnetic loss in a specific frequency range. The minimum reflection loss calculated in decibel units is lower than all the reported value about this material.

Magnetite, whose usual formula representation is $[Fe^{3+}]_{tet}[Fe^{2+}Fe^{3+}]_{oct}O_4$, has high conductivity (half-metal) because of a rapid electron hopping between octahedral ferrous and ferric ions.[23] Maghemite, which has the oxidized structure of $[Fe^{3+}]_{tet}[Fe^{3+}_{5/3}\square_{1/3}]_{oct}O_4$, is an insulator.[23] Magnetite has been proved to exhibit excellent microwave absorption properties on the basis of large dielectric loss aside from magnetic loss.[24] Simultaneously, magnetite has low magnetocrystalline anisotropy energy and resonance frequency. Substitution partial ferrous ions with cobaltous ions can increase both of them and by changing the amount of cobalt atoms, we can even tailor its absorption band. The mixed spinels of magnetite and cobalt ferrite, or called as non-stoichiometric cobalt ferrite, can be obtained facilely in one pot by solvothermal method using ethylene glycol as solvent and sodium acetate as a weak base. Ethylene glycol, whose boiling point is 197 °C, can reduce ferric ions to ferrous ions at a certain temperature.

Solvothermal synthesis method is a low temperature and efficient technique to obtain nanomaterials and the grains can self-assemble into submicrospheres. The wavelength of microwave is in centimeter magnitude. The microwave can easily bypass small obstacle such as nanometer grains, which is the familiar diffraction phenomenon. When the grains gather into spherical balls, they act like "blackbody" greatly enhancing absorption of incident electromagnetic radiation, regardless of frequency or angle of incidence.[17] Also, the crystal structure and size, ingredients and cations distribution together with special geometrical morphology can be modulated by varying the preparation condition and calcination process, and thus changes the microwave absorption capability. From this point of view, the method has demonstrated its superiority over other techniques such as coprecipitation,[10,16,17]electrochemical,[25,26] hydrothermal,[27] combustion[28] and mechanical alloying.[29] Stoichiometric cobalt ferrite has high electrical resistivity, low eddy current and dielectric loss in microwave range. Mixed spinels can not be simply taken as a magnetic absorbent at microwave frequencies and the dielectric loss is comparable with magnetic loss. Thereby the present work is aimed to research into the intrinsic microwave absorption property of non-stoichiometric cobalt ferrite spheres.

2 Experimental

Synthesis method

Cobalt ferrite microsphere were prepared by solvothermal technique reported in reference [30]. Briefly, the synthesis procedure is described as follows: stoichiometric amount of $FeCl_3{\cdot}6H_2O$ (1.35 g, 5 mmol) and $CoCl_2{\cdot}6H_2O$ (0.6 g, 2.5 mmol) was dissolved in ethylene glycol (40 mL) to form a clear solution, followed by addition of anhydrous sodium acetate (3.6 g) and polyethylene glycol 6000 (2.0 g). The mixture was stirred vigorously for 30 min and then sealed in a Teflon-lined stainless-steel autoclave (50 mL capacity). The autoclave was maintained at 200 °C in air oven for 24 hour. Another stainless-steel high pressure autoclave without Teflon liner (100ml capacity) containing 80 ml solution was kept under 300 °C in its heating apparatus with the same duration of time. Then, the autoclaves were cooled down to room temperature naturally. The black products were washed repeatedly with water. They were preserved in ethanol finally for TEM test or dried at 80 °C over 24 hours in air for characterization. The products are denoted by sample A (200 °C) and B (300 °C). Also, sample A was post-treated with calcination at 700 °C for two hours in ambient atmosphere. It is designated as sample C. To investigate the effect of cobalt ratio on the microwave properties, the cobalt to iron atomic ratio in the original ethylene glycol solution was changed from the stoichiometric 1:2 to 1:1, 1:4 and 0 during the next series of experiments. The synthesis temperature was maintained at 200 °C for 24 h. Composites containing magnetic material (75 wt.%) and paraffin wax were mixed uniformly and pressed into toroidal-shaped samples with an outer diameter of 7.00 mm and an inner diameter of 3.04 mm for the measurement of electromagnetic parameters.

Characterization and property measurements

Morphology and composition of samples were characterized by scanning electron microscopy (FESEM，HITACHI S-4800) with an energy-dispersive X-ray spectrometer (EDS) and Transmission electron microscopy (HITACHI H-8100). The Crystallographic analysis and crystallite size of samples were examined by X-ray diffraction (XRD, X' Pert Pro MPD, Cu K_α radiation, λ = 1.54056 Å) operating at a scan rate of 2 °/min. Chemical states of elements and cation locations were investigated by X-ray photoelectron spectroscopy (XPS, PHI Quantera II XPS Scanning Microprobe) with Al Ka radiation (1486.6 eV). The powder spheres were demagnetized before entering into the high vacuum chamber. Magnetic properties were studied by a vibrating sample magnetometer (VSM, Lakeshore 7407, USA) under maximum magnetic field of 1.0 T at room temperature. Scattering parameters (S_{11}, S_{21}) were recorded on an Anritsu 37269D vector network analyzer in the frequency range of 2 -18 GHz. Relative complex permittivity (ε_r) and permeability (μ_r) were obtained from Nicolson-Ross-Weir method.

3 Results and discussion

Crystal structure and morphology

Fig.1 shows the X-ray diffraction pattern of the samples. For sample A and B, which are synthesized at 200°C and 300°C respectively, all the peaks in the pattern can be indexed as cubic spinel $Co_xFe_{3-x}O_4$，wherein x stands for cobalt content and can vary from zero to one. The crystallite size of the samples is extracted from the Debye-Scherrer equation $d = 0.89\lambda/\beta\cos\theta$, where d is the average size of the crystallites, λ is the wavelength of the X-ray source, 1.5406 Å, β is the full width half maximum (FWHM) of the definite diffraction peak in radians, and θ is Bragg angle of the corresponding XRD peak. From the peak data corresponding to (311) plane, the crystallite size of 23 nm (sample A) and 30 nm (sample B) are obtained. It seems reasonable that high-temperature synthesis results in big crystallites. When sample A was calcined at 700°C for two hours, new peaks emerge and they are attributed to the second phase α-Fe_2O_3 (JCPDS No. 33-0664). The morphology of samples was analyzed by FESEM as shown in Fig.2. The micrographs indicate that they are 300-500 nm spheres in dimension and composed of

small primary particles. The particles are packed tightly as an outcome of the attractive magnetic force and instinctive nature to reduce surface energy by aggregation.[24]. Also, Fig.2 (c) and (d) illustrate that spheres B are somewhat smaller and made up of bigger crystallites than A. After calcination, the crystallites in sphere C grow up into bigger one too. The TEM image in Fig.3 corroborates the results again and the inset SAED proves that the spheres A are polycrystalline or composed of small grains.

Magnetic and dielectric properties of spheres

Fig.4 shows the magnetic hysteresis loops measured under a maximum applied field of 1T Oe at room temperature. The saturation magnetization, retention magnetization and coercivity of spheres A are 69.944 emu/g, 29.460 emu/g and 833.81Oe respectively; for B, they are 77.425 emu/g, 38.365 emu/g and 1194.6Oe. Spheres B exhibit better magnetic properties than A,

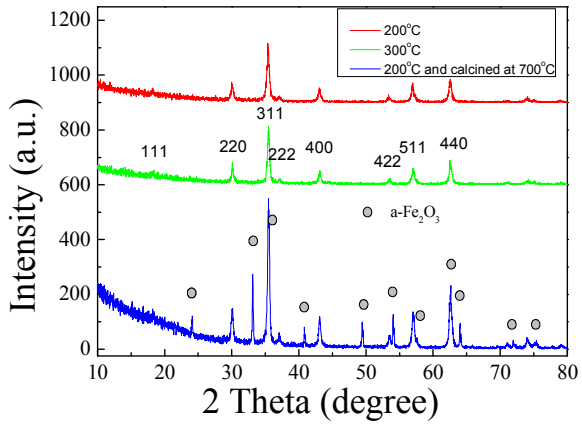

Fig.1 XRD patterns of $Co_xFe_{3-x}O_4$ samples synthesized at 200°C , 300°C and 200°C post-calcined at 700°C for two hours.

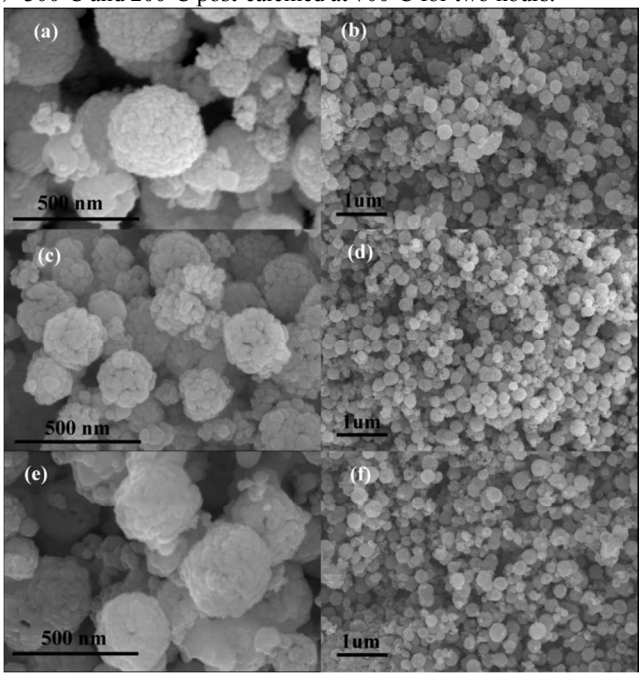

Fig.2 FESEM images of $Co_xFe_{3-x}O_4$ spheres synthesized by solvothermal method at different temperatures：(a) and (b), sphere A, $Co_{0.9}Fe_{2.1}O_4$, 200°C; (b) and (c), sphere B, $Co_{0.74}Fe_{2.26}O_4$, 300°C; (e) and (f), sphere C, sphere A post-treated with calcinations at 700°C for two hours.

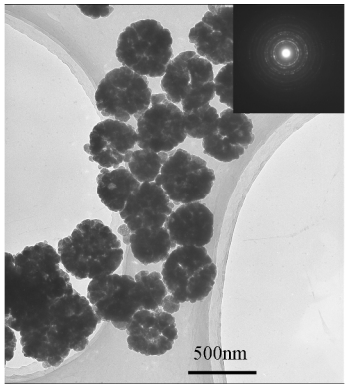

Fig.3 TEM and SAED images of $Co_{0.9}Fe_{2.1}O_4$ spheres (sphere A).

as is expected for the higher synthesis temperature and bigger crystallites. Calcined spheres A (spheres C) exhibit the highest coercivity of 1540.3Oe and the lowest magnetization and retentivity, which are 45.928 emu/g and 25.663 emu/g, respectively. The results can be understood for the reason that hematite shows bad magnetic property. The compositional analysis of the samples is determined by EDS quantification as shown in Table.1. In stoichiometic cobalt ferrite crystal, atomic ratio of oxygen should be 57.14% and this element approximates the value in both spheres. Cobalt element, which should be 14.3%, is actually 12.86% (sphere A) and 10.55% (sphere B). So there is an iron element surplus, although in the original solution the ratio of cobalt to iron atoms is 1:2. The iron atoms in the spheres contain mixed valence due to the reduction effect of ethylene glycol.[30] The reduction effect is enhanced at a higher temperature of 300°C. So, there are more Fe^{2+} ions in sphere B (Table1 and Figure S2). More ferrous ions mean less cobaltous ions. The reason is that the total of them should be nearly half of the ferric ions or one fourth of the oxygen atoms to reach charge balance. The molecular formula of sphere A and B can be decided as $(Co_{0.9}Fe_{0.1})Fe_2O_4$ and $(Co_{0.74}Fe_{0.26})Fe_2O_4$ separately and the cations in parenthese are both bivalent. The redefined molecular formula is derived from calibrating the oxygen atom number to be four and the cobalt atom according to the EDS value (less than 1). So, the iron atom number obtained from EDS is slightly changed.

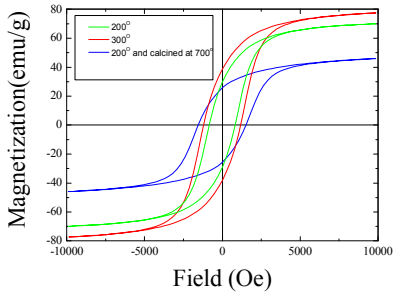

Fig.4 Magnetization hysteresis loops of different $Co_xFe_{3-x}O_4$ spheres synthesized by solvothermal method at 200°C (sphere A), 300°C (sphere B) and 200°C with post-calcination at 700°C for two hours (sphere C).

Fig.5 (a) presents the frequency dispersion of complex

permittivity (ε=ε'-jε") of composites containing 75% (weight ratio) spheres and paraffin wax. As far as composite A and B are concerned, the monotonically descending trend of the real part of dielectric permittivity with frequency is evident. In particular, most of the decrease occurs between 2 GHz and 9 GHz. The imaginary part of composite A is higher than B in the frequency range from 2 GHz to 10 GHz. Despite that, in the frequency range of 10-18 GHz, the ε" spectra of both composites are similar. When spheres A were calcined at 700℃ for two hours (sphere C), the real part of permittivity shows an low value of four. The dielectric constant of paraffin wax is 2.1-2.5, so the actual dielectric constant of spheres C is much lower than as-prepared. Also, the imaginary part of permittivity is near zero indicating little dielectric loss. The real part represents the energy stored during the dielectric polarization whereas the imaginary one is correlated with the energy spent to align dipole moments according to the oscillating electrical field. For microwave absorption purpose, dielectric material should exhibit the highest possible value of ε" at the operational frequency. According to the analysis, the dielectric property of spheres A is the best for microwave attenuation and spheres C is the worst.

Table 1 the weight ratio and atomic ratio of elements (Co:Fe:O) in different cobalt ferrite spheres revealed by the EDS spectra in Figure S1. The redefined molecular formula and the cobalt to iron atomic ratio in EG solution are also shown in the first and the second column respectively.

Redefined molecular formula (synthesis temperature)	Co:Fe in solution	Co in sphere		Fe in sphere		O in sphere		Nominal Co:Fe:O in sphere
	Atomic ratio	Weight ratio (%)	Atomic ratio (%)	Weight ratio (%)	Atomic ratio (%)	Weight ratio (%)	Atomic ratio (%)	Atomic ratio
$CoFe_2O_4$ (200°C)	1:1	27.89	15.83	44.65	26.75	27.46	57.42	$Co_{1.11}Fe_{1.87}O_{4.02}$
$Co_{0.9}Fe_{2.1}O_4$ (sphere A, 200°C)	1:2	22.60	12.86	50.22	30.16	27.18	56.98	$Co_{0.9}Fe_{2.11}O_{3.99}$
$Co_{0.73}Fe_{2.27}O_4$ (200°C)	1:4	18.34	10.39	54.28	32.46	27.38	57.15	$Co_{0.73}Fe_{2.27}O_4$
Fe_3O_4 (200°C)	0	0	0	65.55	35.28	34.45	64.72	$Fe_{2.47}O_{4.53}$
$Co_{0.74}Fe_{2.26}O_4$ (sphere B, 300°C)	1:2	18.38	10.55	55.09	33.37	26.53	56.09	$Co_{0.74}Fe_{2.34}O_{3.92}$

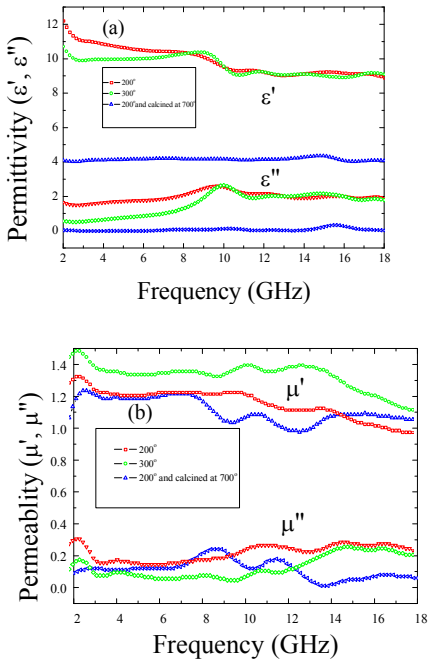

Fig.5 Permittivity (a) and permeability (b) of composites containing different $Co_xFe_{3-x}O_4$ spheres (75% weight ratio) and paraffin wax.

Fig.5 (b) shows the complex permeability (μ=μ'-jμ") as a function of frequency. According to Snoek' limit,[31] the real part of the permeability μ' decreases with increased frequency and the imaginary part of the permeability μ" goes through a broad resonance and decreases afterwards.[1] Their values are high within megahertz frequency but low in gigahertz frequency range. The value of μ' is the highest with composite B and the lowest with C, which coincides with the static magnetic properties. When magnetic loss is concerned, cobalt ferrite attenuates EMW by the mechanism of magnetic hysteresis loss, domain-wall resonance, and electron spin resonance. Considering the grain size in our spheres and microwave frequencies, only the latter two resonances take effect. There exists a peak around 2.5 GHz in both real and imaginary part of permeability spectra. This can be attributed to domain wall resonance.[32] The resonance frequency, which is sensitive to the grain size, is the lowest with composite A (2.5 GHz) and the highest with C (8.8 GHz). For composite B, the resonance frequency is a little higher than A (2.6 GHz). Another broad peak appears at 14.5-17GHz with composite A and B, and around 9.5 GHz with C. The peak may be ascribed to spin rotational resonance, which is composition and structure sensitive.[32,33] The resonance frequency f is proportional to the anisotropy field H_A and can be expressed by the equation $f = \gamma H_A/2\pi$, where g is the gyromagnetic ratio and H_A is the crystal anisotropy field.[24,32] H_A can be described as $H_A = 2K/\mu_0 M_S$, where K is crystalline anisotropy constant and $K = 2.7\times10^5$ J/m^3 for cobalt ferrite.[34] Cobalt ferrite possesses the highest anisotropy constant and moderate M_S value in cubic spinel ferrites. The spin rotational resonance should appear at a high frequency of 34.7 GHz. Actually our spheres are the mixture of cobalt ferrite and magnetite. The calculated resonance frequency is not accurate using the value of bulk material. There also exist some other

small peaks and the spectra fluctuate. In comparison with composite B, A has a higher value of μ" in the 2-15 GHz range and almost the same value in the 15-18 GHz range. The results prove again Janis' assertation that low density cobalt ferrite grains have a higher imaginary part of permeability.[11] He also concluded that both the real and imaginary part of permittivity are higher for high density grains. This is not true with our samples. The reason lies partly in the morphology difference between the submicron spheres and the separate grains of *ca.* 45 nm. The spherical structure composed of grains behaves like a "black hole" to a certain degree when EMW transmits into it.[17]

microwave absorption properties of spheres

When used as an absorbent of radar EMW at centimeter wavelength (2-18 GHz), the composite layer is located between free space and metal plate. The input impendence Z_{in} of the absorbent can be expressed by [8]

$$Z_{in} = Z_0\sqrt{\frac{\mu_r}{\varepsilon_r}}\tanh\left[\frac{j2\pi d}{\lambda}\sqrt{\varepsilon_r\mu_r}\right]$$

where Z_0 is wave impedance of free space (376.7 Ω), ε_r and μ_r are respectively the relative complex permittivity and permeability of the composite medium, λ is EMW wavelength in free space, and d is thickness of composite layer. The reflection loss of the composite can be calculated by the formula

$$R.L. = 20\log\left|\frac{Z_{in}-Z_0}{Z_{in}+Z_0}\right|$$

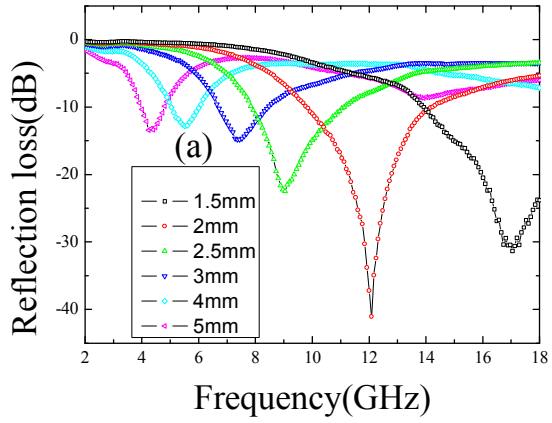

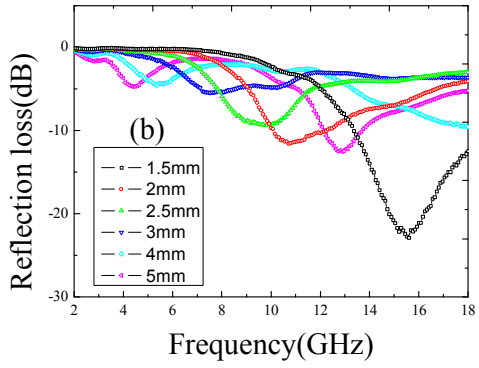

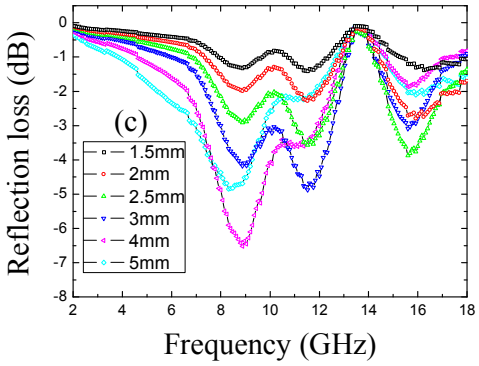

Fig.6 Reflection loss of composites containing $Co_xFe_{3-x}O_4$ spheres (75% weight ratio) fabricated at: (a) 200°C, sphere A, (b) 300°C, sphere B and (c) 200°C and then calcined at 700°C, sphere C, and paraffin wax with various thickness.

Fig. 6 shows the reflection loss computed from the complex permittivity and permeability of the composites which contain different spheres (75% mass ratio) and paraffin wax. For composite A in 1.5 mm thickness, the minimum reflection loss of -31.330 dB occurs at 17.04 GHz and the frequency bandwidth of less than -20 dB (99% absorbed) is between 16 GHz and an upper limit exceeding 18 GHz. At the thickness of 2 mm, the magnitude of absorbing peak reaches -41.089 dB at 12.08 GHz with 1.36 GHz bandwidth (less than -20 dB). For a 1.5 mm thick layer of composite B, the minimum RL value of -22.906 dB appears at 15.6 GHz and the reflectivity of less than -20 dB is over the range of 14.8 - 16.16 GHz. Increasing the thickness results in the shift of absorption band to lower frequency field. For composite C, microwave attenuation is mainly caused by magnetic loss and the reflection value is greater than -7 dB. The three attenuation peaks correspond to the μ" frequency dependence profile and do not move with absorber thickness. The results indicate that spheres A dissipate the microwave energy more efficiently than the others.

To achieve better results in microwave absorption, the impedance matching between free space and the composite material should be fulfilled, i.e. $Z_{in} = Z_0$. The requirement can be fulfilled when the complex permittivity matches the complex permeability at a particular frequency for a certain thickness.[13,18,35,36] The real parts of them may be much different. So, the applicable solution is to increase both the imaginary parts of complex permittivity and permeability. The reflection loss formula indicates that when the real part of normalized input impedance Z_{in}/Z_0 approach unity and the imaginary part of Z_{in}/Z_0 is close to zero, large reflection loss can be obtained. Table 2 shows the relative input impedance Z_{in}/Z_0 for different samples when their reflection loss is the minimum. For composite A, when the real part reaches the value 1, the imaginary part is very low and the calculated reflection loss turns out to be much low. For composite B, when the real part approaches 1, the imaginary part is a little high. The former increases with frequency and the latter decreases until the optimal parameters are reached, but the calculated loss is higher than composite A. Composite C is similar with composite B in this respect. However, the discrepancy towards ideal Z_{in}/Z_0 is even bigger and the loss is doubtlessly the highest one.

Table.2 calculated relative input impendance and the matching parameters of the three composites when the reflection loss is the minimum.

sphere/minimum loss /frequency/thickness	Z_{in}/Z_0
A,-41.089dB, 12.08GHz, 2mm	1.01780092626113+0.0000258425611579741j
B,-22.906dB, 15.6GHz, 1.5mm	1.15405770955897+0.00534003050567181j
C,-6.525dB, 8.88GHz, 4mm	2.78055460454623+0.118730169950067j

XPS determination of cation sites and discussion

The spheres are further investigated by X-ray photoelectron spectroscopy (XPS), which can identify and quantify elemental composition and the chemical states of the detected elements, even their local environments. The C1s binding energy of the minor hydrocarbon contaminants in the vacuum is taken as 284.6 eV. [37] To eliminate the charging effect, all binding energies have been corrected with reference to it. Fig.7 (a) illustrates a broad scan XPS spectrum (from 0 to 1100 eV) of different spheres which confirming again the elements of iron, cobalt and oxygen, similarly to EDS analysis. Furthermore, detailed 2p spectra of iron and cobalt elements in different spheres are shown in Fig.7 (b) and (c). The peak heights are different as a result of scattering effect created by the strength discrepancy of intrinsic magnetic field. Their spectral envelopes are composed of two main peaks corresponding to $2p_{3/2}$ and $2p_{1/2}$ contributions. In Fig.7 (b), a shake-up satellite is observed between $Fe2p_{3/2}$ and $Fe2p_{1/2}$ peak in spheres C spectrum and spheres A and B have no satellites between them. The satellite is indicative of existing a-Fe_2O_3.[38] Spheres C contain only ferric ion and the others comprise both ferric and ferrous ions. On account of higher binding energy of ferric than ferrous ion, a chemical shift can be discerned comparing $Fe2p_{3/2}$ peak in spheres C spectrum with A. We do not deconvolute the high spin Fe2p spectra through multiplet splitting patterns because the binding energy complexity associated with overlapping subspectra of ferric and ferrous ions. It is hard to discriminate them qualitatively, much less determine their location. Fig.7 (c) shows that the $Co2p_{3/2}$ and $Co2p_{1/2}$ main binding energies are observed at 781.5 ± 0.1 eV and 797.3 ± 0.1 eV, respectively with their corresponding satellites.[39] The $Co2p_{3/2}$ satellite confirms the cobaltous ion, excluding the possibility of trivalence state.[40,41] As can be seen from Fig.7 (d) - (f), by using least squares routine following subtraction of the Shirley background, The envelope can be split into three components with respective fixed binding energy, namely the octahedral site location of cobalt ions at 780.6 eV, the tetrahedral site at 782 eV and the satellite at 786 eV. In $2p^{1/2}$ spectrum, the binding energy of cobaltous ion in tetrahedral site is reported 1.1 eV higher than octahedral site.[42] In our case, the binding energy shift in $2p^{3/2}$ spectrum is 1.4 eV, similarly with reference [43]. Closer examination of peak intensities in the three spectra does indicate that the cobalt ions move from octahedral to tetrahedral sites. The quantitive analysis based on relative peak areas show that 47.5% cobalt ions locate in octahedral site in sphere A, 23% in sphere B and 18% in sphere C. Thus the ferric ions migrate in the opposite direction at a higher synthesis or calcination temperature.[44] Also, ion exchange between ferrous and ferric ions happens in the same way in spheres A and B because the cobaltous ions and the ferrous ions have the same valence and nearly the same ionic radii, which are 0.72 Å and 0.74 Å respectively in octahedral coordination. Contrastively, it is smaller with ferric ion (0.645 Å).[45]

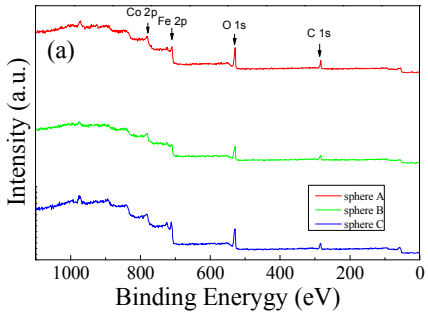

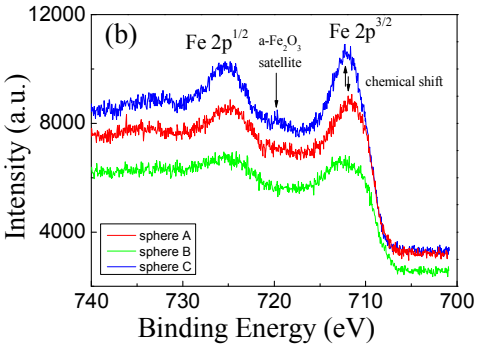

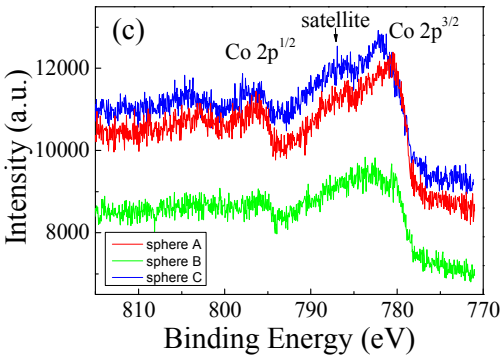

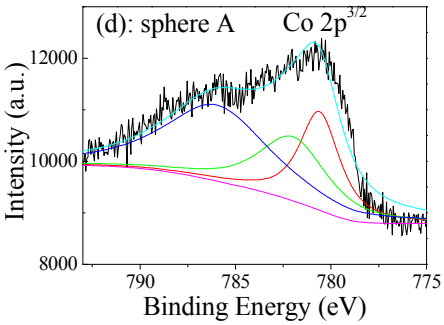

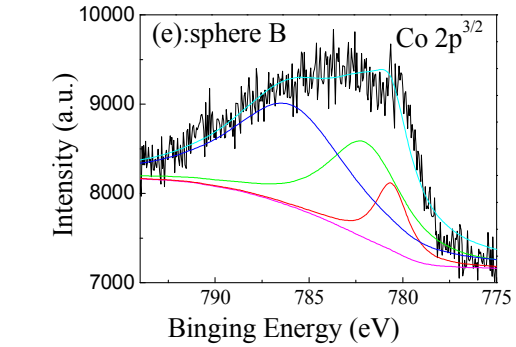

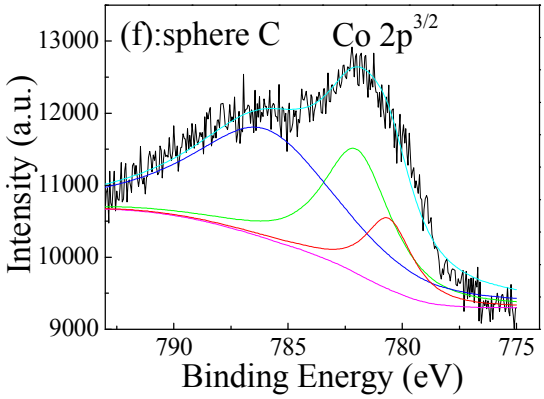

Fig.7 XPS spectra of (a) broad scan of different $Co_xFe_{3-x}O_4$ spheres; (b) and (c) slow scan of Co and Fe elements; (d) - (f) Co $2p^{3/2}$. Spectra of spheres A, B and C are fitted by Xpspeak41 software with a Shirley background subtraction and 80%/20% Lorentizian/Gaussian peak shape.

Cobalt ferrite and magnetite have inverse spinel structure with Fe^{3+} ions equally distributed in tetrahedral interstitial sites (A site) and octahedral interstitial sites (B site), and Co^{2+} or Fe^{2+} ions in B sites. There are 8 A sites and 16 B sites occupied by metal cations in addition to 32 oxygen atoms in a cubic unit cell. Its geometry is shown in Fig.8. The dielectric and magnetic properties are correlated to the distribution of the transition metal ions among the cationic sites.[46] In general, the complex permittivity in ferrites is attributed to four types of polarization (interfacial, dipolar, ionic and electronic).[12] At gigahertz frequencies, only the third and fourth polarizations prevail. In sphere A, which is composed of small grains, most of Co^{2+} and Fe^{2+} ions occupy the octahedral sites,[44]The distance between the cations in adjacent B sites equals $\sqrt{2}a/4$ (0.2967 nm, a is the lattice parameter from $CoFe_2O_4$, a=0.8392nm, JCPDS 22-1086), which is smaller than the A-A site distance $\sqrt{3}a/4$ (0.3634 nm) and the A-B site distance$\sqrt{11}a/8$ (0.3479 nm).[47,48]Also, the degree of covalency for B site cations is known to be lower than that of A site cations.[47,48] Electron transfer is easy between Fe^{3+} and Fe^{2+} in adjacent octahedral sites. The electrical conductivity and polarizability of mixed ferrites are greatly enhanced.[23] The larger the number of $Fe^{2+}\leftrightarrow Fe^{3+}$ ion pairs, the higher would be the dielectric constant.[12,24,49,50]

In sphere B, some Co^{2+} and Fe^{2+} ions enter into the tetrahedral site due to higher synthesis temperature. The ferric and ferrous ions are partly separated. Yet sphere B still has more ferrous ions in octahedral sites. So there is another affective factor, the crystallinity of the sphere. Well-crystallized sphere are composed of big crystallites which has few defects, such as surface dangling bonds, oxygen and metal interstitials and vacancies, resulting in small imaginary permittivity value. Even the slightest chemical and physical change may have a dramatic effect on the dielectric properties. So, the real and imaginary parts of dielectric permittivity are lower for spheres B in comparison with A. At a higher frequency of 9-10 GHz, the ionic polarization cannot follow the variational electric field. The real and imaginary part of permittivity change inversely. The complex permittivity dispersions of spheres A and B show a fair resemblance beyond this frequency due to contribution mainly from electronic polarization. In spheres C, all the Fe^{2+} ions are oxidized to Fe^{3+} and give rise to new material α-Fe_2O_3. Co^{2+} ions locate mostly in thermodynamically unstable tetrahedral sites and Fe^{3+} ions in octahedral sites.[45] The cation migration does render cobalt ferrite crystal towards normal spinel structure. However, there exist no $Fe^{2+}\leftrightarrow Fe^{3+}$ ion pairs and very few defects. The real part of dielectric permittivity is low and the imaginary part is near zero. In cubic ferrite spinels, the ferrimagnetic order originates from the super exchange interaction between the metal ions in the tetrahedral and octahedral sublattices. The magnetic moment of Co^{2+}, Fe^{2+} and Fe^{3+} ion is 3 μ_B, 4 μ_B and 5 μ_B respectively (μ_B herein is the Bohr magneton). Spheres B display better static magnetic properties than A as a result of two contradicting factor. One is the bigger crystallite size (multidomain) leading to a decline of the saturation magnetization. However, Fe^{2+} and Co^{2+} location changes from octahedral to tetrahedral sites cause the higher moment value per formula unit, which is the cancellation result of two sublattices. Obviously, the second factor takes a leading role. In another point of view, sphere A and B can be taken as a mixture of cobalt ferrite and magnetite and the latter displays higher saturation magnetization value than the former in bulk material. Spheres B have more Fe^{2+} ions and thus more magnetite ratio than A. As for spheres C, paramagnetic hematite makes the overall magnetic property worse although the cobalt ferrite portion may improve its own magnetic property after calcination.

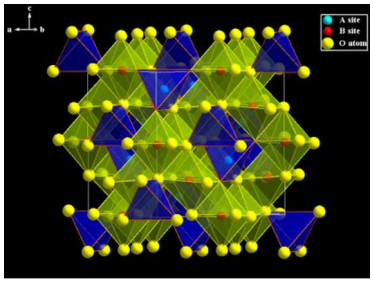

Fig.8 Tetrahedral（in blue）interstitial positions (A site) and octahedral (in yellow-green) interstitial positions (B site) in a crystal unit cell of cobalt ferrite.

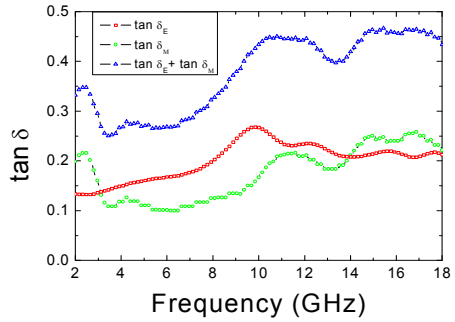

Fig.9 Frequency dependence of dielectric dissipation factor tan δ_E, magnetic dissipation factor tan δ_M, and tan δ_E + tan δ_M of composite A.

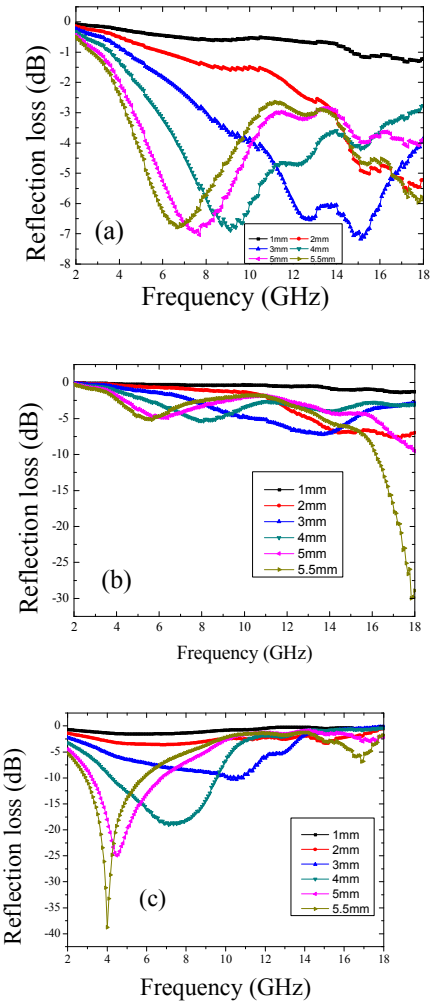

Fig.10 Reflection loss of composites containing $Co_xFe_{3-x}O_4$ spheres ($CoFe_2O_4$, (a), $Co_{0.73}Fe_{2.27}O_4$, (b), and Fe_3O_4, (c), which are all fabricated at 200°C for 24h, 75% weight ratio) and paraffin wax with various thickness.

Comparison of magnetic and dielectric loss contributions and microwave absorption properties of spheres with different cobalt ratio

In order to investigate the contribution of different microwave attentuation mechanism in composite A, the dielectric and magnetic dissipation factors (tan $\delta_E = \varepsilon''/\varepsilon'$, tan $\delta_M = \mu''/\mu'$) are calculated separately and shown in Fig. 9. Both the dielectric and magnetic losses contribute somewhat to the microwave absorption. Dielectric loss factor is higher than magnetic loss in the frequency range of 3 - 14 GHz. The total loss factor is large in the frequency range of 10 -18 GHz. Consequently, sphere A shows better microwave absorption property in the second half of X and Ku bands.[11,35] The matching thickness is low (1.5 - 2 mm).

The magnetocrystalline anisotropy constant of magnetite is much lower than cobalt ferrite, which contains additional element cobalt. Sequentially the spin rotational resonance frequency is reduced. We can adjust the band of minimum absorption by changing cobalt ferrite ratio in the mixed ferrites. During the next experiments, the cobalt to iron atomic ratio in the original ethylene glycol solution were changed from the stoichiometric 1:2 to 1:1, 1:4 and 0. The EDS analysis shows that the fabricated spheres are $CoFe_2O_4$, $Co_{0.73}Fe_{2.27}O_4$, and Fe_3O_4 respectively (Table 1 and Figure S1), and $Co_{0.73}Fe_{2.27}O_4$ contains more cobalt ratio in spheres than in solution, indicating that the ferrous ions reduced from ferric ions by EG are not sufficient. XRD and FESEM characterization in Figure S3-S5 shows that all the spheres are ferrites. The sphere is better crystallized for low cobalt ratio, and magnetite is the best one. The crystallites are calculated to be 16nm, 25nm and 39nm in size respectively. VSM measurements show that the mass magnetization value is increased with decreased cobalt ratio and the coercivity field first increase and then decrease with descending cobalt ratio. The complex permittivity and permeability are shown in Figure S6. Magnetite, just as formerly described, display the highest real permittivity value because a lot of $Fe^{2+} \leftrightarrow Fe^{3+}$ pairs exist. Its value (6-8) is lower than sphere A (9-12) because of the low pressure moulding in this batch of toroidal-shaped samples. Due to similar reason, we find that sphere $Co_{0.73}Fe_{2.27}O_4$ display higher imaginary permittivity value than the others but is inferior to sphere B ($Co_{0.74}Fe_{2.26}O_4$). For $CoFe_2O_4$ sphere, there are no peaks in the dispersion curve of imaginary permittivity due to the lack of $Fe^{2+} \leftrightarrow Fe^{3+}$ pairs. The magnetite sphere should exhibit high imaginary permittivity value but actually does not because of high crystallinity. Interestingly, it exhibits high real and imaginary permeability value in the low frequency range because of spin rotational resonance. The reflection loss for composite containing nearly stiochiometric cobalt ferrite spheres (75% mass ratio) is shown in Fig.10 (a) and the microwave absorption property is not good. For $Co_{0.73}Fe_{2.27}O_4$ composite, the lowest reflection loss is -30 dB at 17.84 GHz and the frequency range below -20 dB is calculated to be 0.96 GHz (Fig.10 (b)). For magnetite composite shown in Fig.10 (c), the lowest reflection loss is -38.773 dB at 4 GHz and the reflection loss below -20 dB is in the range of 3.68 - 4.4 GHz. Both of the minimum loss values are obtained when the composite thickness is 5.5mm. Though the properties are not good enough, we can prove the hypothesis mentioned at the beginning of this section. The ratio of cobalt in the ferrite not only affects the resonance frequency, but also change the crystallinity of the spheres, or defects, and ultimately the dielectric and magnetic property are tuned together with the microwave absorption properties. Comparatively, magnetite spheres (40% volume fraction in paraffin wax) in reference [24] exhibit excellent performance (-45.2 dB) at 4.67 GHz and the matching thickness is a little low (4 mm).[14] Besides, their sphere distribution is in a wide range of 200 nm – 1μm. The magnetite spheres can be used in microwave absorption of C and the first half of X bands. There are other reports [13,15] about

uniform magnetite spheres of 300 nm. The magnetic loss factor is much bigger in the range of 2 -10 GHz and 16 -18 GHz. However, the dielectric loss factor is small and the EMW absorption capability is thus limited. Comparing with all the $Co_xFe_{3-x}O_4$ spheres, sphere A features superb absorbing performance, high frequency of absorbing band, and thin thickness as a result of the synergistic effect of both losses. Its property is correlated closely with the proper value of cobalt ratio (0.9) in mixed spinels.

4 Conclusions

$Co_xFe_{3-x}O_4$ spheres, mixed spinels of magnetite and cobalt ferrite, are synthesized in EG solution of stoichiometic cations at varied temperature (200°C, 300°C) and under post-treatment of calcination at 700 °C. Comparison between 200 °C ($Co_{0.9}Fe_{2.1}O_4$) and 300 °C ($Co_{0.74}Fe_{2.26}O_4$) synthesis reveals that at a higher temperature: more ferric ions are reduced to ferrous ions and some of the ferrous ions migrate from octahedral to tetrahedral sites; the grains are bigger and the defects are greatly reduced; the dielectric and microwave absorption properties get worse. However, the static magnetic parameters, such as saturation magnetization, retentivity and coercivity, are larger with 300 °C synthesized spheres. After calcination, hematite emerges as a result of cobalt deficiency and oxidization of ferrous ions. The spheres display the highest coercivity and the lowest saturation magnetization. The dielectric loss is little as a result of disappeared $Fe^{2+} \leftrightarrow Fe^{3+}$ pairs and a decrease in defects. This work also researches into the ingredient of cobalt on the minimum reflection loss value of spheres and corresponding frequency band, offering an alternative way to tailor the microwave absorption properties of magnetite by introduction of cobalt ions without altering the spinel structure. Most noteworthy is, the cobalt ratio in mixed spinels can change the crystallinity of the spheres and the dielectric properties. Among the spheres, the $Co_{0.9}Fe_{2.1}O_4$ sphere exhibits the best microwave absorption performance. More contribution of dielectric loss can be appreciated than magnetic loss in the 3 - 14 GHz range. The product derived from dual losses enable the non-stoichiometric cobalt ferrite a promising microwave absorptive material in X and Ku bands. The work explores the relationship of the sphere fabrication condition, ingredients and structure towards its microwave absorption property.

Acknowledgements

This work was supported by National Natural Science Foundation of China (21371023，50972017) and the Research Fund for the Doctoral Program of Higher Education of China (20101101110026). We owe special thanks to professor Maosheng Cao in electromagnetic parameter measurements.

Notes and references

1 Qiang, C.; Xu, J.; Zhang, Z.; Tian, L.; Xiao, S.; Liu, Y.; Xu, P. *Journal of Alloys and Compounds* **2010**, *506*, 93.

2 Zhu, Y.-F.; Zhang, L.; Natsuki, T.; Fu, Y.-Q.; Ni, Q.-Q. *Acs Applied Materials & Interfaces* **2012**, *4*, 2101.

3 Sun, G.; Dong, B.; Cao, M.; Wei, B.; Hu, C. *Chemistry of Materials* **2011**, *23*, 1587.

4 Saini, P.; Choudhary, V.; Vijayan, N.; Kotnala, R. K. *Journal of Physical Chemistry C* **2012**, *116*, 13403.

5 Bregar, V. B. *Ieee Transactions on Magnetics* **2004**, *40*, 1679.

6 Ma, Z.; Cao, C.; Yuan, J.; Liu, Q.; Wang, J. *Applied Surface Science* **2012**, *258*, 7556.

7 Tsai, C. S.; Su, J. *Applied Physics Letters* **1999**, *74*, 2079.

8 Xu, P.; Han, X.; Jiang, J.; Wang, X.; Li, X.; Wen, A. *Journal of Physical Chemistry C* **2007**, *111*, 12603.

9 Zhang, L.; Li, Z. *Journal of Alloys and Compounds* **2009**, *469*, 422.

10 Fannin, P. C.; Marin, C. N.; Malaescu, I.; Stefu, N.; Vlazan, P.; Novaconi, S.; Sfirloaga, P.; Popescu, S.; Couper, C. *Materials & Design* **2011**, *32*, 1600.

11 Janis, A.; Olsson, R. T.; Savarge, S. J.; Gedde, U. W.; Klement, U. In *Behavior and Mechanics of Multifunctional and Composite Materials 2007*; Dapino, M. J., Ed. 2007; Vol. 6526, p P5261.

12 Sivakumar, N.; Narayanasamy, A.; Chinnasamy, C. N.; Jeyadevan, B. *Journal of Physics-Condensed Matter* **2007**, *19*.

13 Jia, K.; Zhao, R.; Zhong, J.; Liu, X. *Journal of Magnetism and Magnetic Materials* **2010**, *322*, 2167.

14 Ni, S.; Wang, X.; 3Zhou, G.; Yang, F.; Wang, J.; He, D. *Journal of Alloys and Compounds* **2010**, *489*, 252.

15 Zhao, R.; Jia, K.; Wei, J.-J.; Pu, J.-X.; Liu, X.-B. *Materials Letters* **2010**, *64*, 457.

16 Maqsood, A.; Khan, K. *Journal of Alloys and Compounds* **2011**, *509*, 3393.

17 Fu, W.; Liu, S.; Fan, W.; Yang, H.; Pang, X.; Xu, J.; Zou, G. *Journal of Magnetism and Magnetic Materials* **2007**, *316*, 54.

18 Chen, K.; Xiang, C.; Li, L.; Qian, H.; Xiao, Q.; Xu, F. *Journal of Materials Chemistry* **2012**, *22*, 6449.

19 Che, R. C.; Zhi, C. Y.; Liang, C. Y.; Zhou, X. G. *Applied Physics Letters* **2006**, *88*.

20 Prasanna, G. D.; Jayanna, H. S.; Lamani, A. R.; Dash, S. *Synthetic Metals* **2011**, *161*, 2306.

21 Gandhi, N.; Singh, K.; Ohlan, A.; Singh, D. P.; Dhawan, S. K. *Composites Science and Technology* **2011**, *71*, 1754.

22 Xi, L.; Wang, Z.; Zuo, Y.; Shi, X. *Nanotechnology* **2011**, *22*.

23 Fujii, T.; De Groot, F.; Sawatzky, G.; Voogt, F.; Hibma, T.; Okada, K. *Physical Review B* **1999**, *59*, 3195.

24 Ni, S. B.; Sun, X. L.; Wang, X. H.; Zhou, G.; Yang, F.; Wang, J. M.; He, D. Y. *Materials Chemistry and Physics* **2010**, *124*, 353.

25 Sartale, S. D.; Lokhande, C. D. *Ceramics International* **2002**, *28*, 467.

26 Mazario, E.; Morales, M. P.; Galindo, R.; Herrasti, P.; Menendez, N. *Journal of Alloys and Compounds* **2012**, *536*, S222.

27 Pervaiz, E.; Gul, I.; Anwar, H. *Journal of superconductivity and novel magnetism* **2013**, *26*, 415.

28 Liu, Y.; Zhang, Y.; Feng, J.; Li, C.; Shi, J.; Xiong, R. *Journal of Experimental Nanoscience* **2009**, *4*, 159.

29 Sani, R.; Beitollahi, A.; Maksimov, Y. V.; Suzdalev, I. *Journal of materials science* **2007**, *42*, 2126.

30 Deng, H.; Li, X. L.; Peng, Q.; Wang, X.; Chen, J. P.; Li, Y. D. *Angewandte Chemie-International Edition* **2005**, *44*, 2782.

31 Kim, S. S.; Kim, S. T.; Ahn, J. M.; Kim, K. H. *Journal of Magnetism and Magnetic Materials* **2004**, *271*, 39.

32 Xie, J.; Han, M.; Chen, L.; Kuang, R.; Deng, L. *Journal of Magnetism and Magnetic Materials* **2007**, *314*, 37.

33 Kwon, H. J.; Shin, J. Y.; Oh, J. H. *Journal of Applied Physics* **1994**, *75*, 6109.

34 Virden, A.; Wells, S.; O'Grady, K. *Journal of Magnetism and Magnetic Materials* **2007**, *316*, E768.

35 Ji., X.; Lu., M.; Ye., F.; Zhou., Q. *Journal of Materials Science Research* **2013**, *2*, 35.

36 Mandal, A.; Das, C. K. *Journal of Electronic Materials* **2013**, *42*, 121.

37 Temesghen, W.; Sherwood, P. *Analytical and bioanalytical chemistry* **2002**, *373*, 601.

38 McIntyre, N.; Zetaruk, D. *Analytical Chemistry* **1977**, *49*, 1521.

39 Gandubert, A.; Legens, C.; Guillaume, D.; Rebours, S.; Payen, E. *Oil & Gas Science and Technology-Revue de l'IFP* **2007**, *62*, 79.

40 Davison, N.; McWhinnie, W. R.; Hooper, A. *Clays Clay Miner* **1991**, *39*, 22.

41 Borod'Ko, Y. G.; Vetchinkin, S.; Zimont, S.; Ivleva, I.; Shul'Ga, Y. M. *Chemical Physics Letters* **1976**, *42*, 264.

42 Mekki, A.; Holland, D.; Ziq, K.; McConville, C. *Journal of non-crystalline solids* **1997**, *220*, 267.

43 Wang, W.; Yang, H.; Xian, T.; Jiang, J. *Materials Transactions* **2012**, *53*, 1586.

44 Franco, A. *Applied Physics Letters* **2010**, *96*, 172505.

45 O'Neill, H. S. C.; Navrotsky, A. *American Mineralogist* **1983**, *68*, 181.

46 Sivakumar, N.; Narayanasamy, A.; Shinoda, K.; Chinnasamy, C. N.; Jeyadevan, B.; Greneche, J. M. *Journal of Applied Physics* **2007**, *102*.

47 Ponpandian, N.; Balaya, P.; Narayanasamy, A. *Journal of Physics-Condensed Matter* **2002**, *14*, 3221.

48 Abbas, Y. M.; Mansour, S. A.; Ibrahim, M. H.; Ali, S. E. *Journal of Magnetism and Magnetic Materials* **2012**, *324*, 2781.

49 Alcantara, G. B.; Paterno, L. G.; Fonseca, F. J.; Pereira-da-Silva, M. A.; Morais, P. C.; Soler, M. A. G. *Physical chemistry chemical physics : PCCP* **2013**, *15*, 19853.

50 Zhang, H. J.; Liu, Z. C.; Ma, C. L.; Yao, X.; Zhang, L. Y.; Wu, M. Z. *Materials Science and Engineering B-Solid State Materials for Advanced Technology* **2002**, *96*, 289.

Number of ferrous and ferric pairs in adjacent octahedral sites determines the real part of permittivity.

Cobal ratio in mixed spinels determines the crystallinity or number of defects, and ultimately the imaginary part of permittivity.

At higher synthesis or calcination temperature, some cobaltous and ferrous atoms migrate from octahedral to tetrahedral sites.